Proceedings of the Twenty-seventh (2017) International Ocean and Polar Engineering Conference **www.isope.org**
San Francisco, CA, USA, June 25-30, 2017

ISBN 978-1-880653-97-5; ISSN 1098-6189

Vortex Induced Vibration of Riser with Low Span to Diameter Ratio Buoyancy Modules

Dixia Fan[1], Michael S. Triantafyllou[1]*
1 Department of Mechanical Engineering, Massachusetts Institute of Technology.
Cambridge, MA, USA

ABSTRACT

Using an array of high speed cameras and underwater tracking method, we experimentally investigated the flexible cylinder with buoyancy modules undergoing VIV (module to bare cylinder diameter and length ratio of 3.2 and 1; module aspect ratio of 1; coverage ratio of 100% and 50%). It reveals interesting results that the riser will experience bi-frequency and bi-modal vibration due to the excitation from both buoyancy modules and bare cylinder. Based on the coverage ratio and flow condition, when buoyancy modules induced motion dominates the response, the model experiences a small value of reduced frequency down to 0.085 and large vibration amplitudes up to 3.8 riser diameter. Besides, the generation of traveling wave patterns, combined cross-flow and in-line trajectory and a comparison between flexible cylinder model and corresponding rigid model hydrodynamic database will be presented.

KEY WORDS: VIV; flexible riser; buoyancy module; optical measurement;

INTRODUCTION

Mitigating vortex induced vibration (VIV) is one of the key design considerations for the offshore riser and pipeline system. VIV may lead to large fatigue damage and hence system failures. Therefore a significant research effort has been devoted into the understanding of VIV mechanism, such as Xu (2013). One of the key factors that decide VIV response is the structure shape, and, as a matter of fact, sometimes even a small change of the shape will largely affect the vortex formation pattern and hence coupled structural response.

For risers used in the deep water (larger than 1000m), staggered buoyancy modules will be often installed to help providing additional lift force and therefore avoiding the excessive tension load in the riser, discussed by Li, et al. (2011). Meanwhile, buoyancy modules have also been widely used to maintain a lazy wave format for the riser system, shown by Jhingran, et al. (2012). However, because of its larger diameter (normally 2.5-5 times larger than riser diameter), the vortex formation may largely change behind the structure hence the different VIV response for the riser with buoyancy modules, compared to the bare risers. Questions therefore have been raised by Lie, et al. (1998), Vandiver, et al. (2003) and Rao, et al. (2013), such as whether the dynamic response will be dominated by the riser induced or buoyancy modules induced motion, or how the different diameter ratio, length ratio and coverage ratio between the buoyancy modules and riser will affect the dynamic response, etc.

In the previous research, Vandiver, et al. (2003) and Rao, et al. (2013) conducted experiments on the flexile cylinder with buoyancy modules (aspect ratio from 4 to 6), and this allows the modeling of the riser and buoyancy module simply as staggered cylinders with smaller and larger diameters, such as by Triantafyllou, et al. (1999). However, this principle does not apply to the new form of buoyancy modules at an aspect ratio of 1, because the hydrodynamics, the vortex shedding, will be significantly altered for the cylinder with small aspect ratio, shown by Javadi (2014).

In the current research, the flexible cylinder model with buoyancy modules are experimentally tested in the MIT Tow Tank for two different coverage ratios. And using underwater optical tracking methods developed by Fan, et al. (2016) with an array of high speed cameras, the VIV motion of the model is accurately captured in both high temporal and spatial resolution.

The experimental result reveals interesting phenomena that the riser will experience bi-frequency and bi-modal vibration due to the excitation from both buoyancy module and bare cylinder. Based on the coverage ratio and flow condition, when buoyancy module induced motion dominates the response, the model experiences a low reduced frequency number, down to values of 0.085 and a large vibration amplitude up to 3.8 riser diameter. Additionally, the generation of traveling wave patterns, combined cross-flow and in-line trajectory will be presented and corresponding rigid model hydrodynamic database constructed by Le Garrec, et al. (2016) will be also used to explain the phenomena.

EXPERIMENT DESCRIPTION

Model Description.
The shape of the modules used in the experiments is the rigid circular

cylinder with aspect ratio of 1. And module to riser diameter and length ratios are chosen to be 3.2 and 1. Riser models with two different coverage ratios (length of the riser section with buoyancy modules to the total riser length) of 100% and 50% are constructed and tested for different velocities. The core flexible riser model is molded via urethane rubber with embedded fishing line that provides additional axial strength while keeping a low bending stiffness. The attached buoyancy modules are made by low density polyethylene cylinder and then stick on the riser model in a staggered configuration. The following Fig.1 shows the two models used in the current experiments.

Fig. 1 Two riser models with buoyancy modules of 100% (top) and 50% (bottom) coverage ratio (length of the riser section with buoyancy modules to the total riser length). Black and white paint is used as the marker for motion tracking in the experiment.

Compared to the applied tension, the bending stiffness of the urethane rubber model is considered a negligible contribution to the model natural frequency and modal shape, and namely the model exerts a string-like vibrational behavior. For the current research, the diameter and length of the buoyancy modules (D and L) and the riser between two buoyancy modules (d and l) are fixed with aspect ratio of the buoyancy module L/D picked to be 1.0, and the model length ratio $Lr = L/l = 1.0$ and $Dr = D/d = 3.2$. We need to mention that the diameter ratio Dr is carefully picked as a non-integer to avoid potential mixture of the vortex shedding frequencies and the higher-order harmonics of the riser and buoyancy module. The detailed model parameters are listed in the following table 1.

Table 1. Model Properties

Parameter	Model 1	Model 2
Total Length (m)	1.98	1.98
Coverage Ratio	100%	50%
	Riser	B-Module
Outer Diameter (mm)	12	38.1
Section Length (mm)	38.1	38.1
Mass per unit length in air (kg/mm)	0.1561	1.2059

Experimental Setup.

The current experiment was performed at the MIT Tow Tank, and the total setup is shown in the Fig.2.

Two foil shape holders are fixed on the supporting beam with the model installed on the bottom of the holder that allows tension adjustment. 4 cameras are installed over 80d downstream of the model to measure Cross-Flow (CF) vibration while 6 cameras are installed 50d above the model to measure In-Line (IL) vibration. At the same time, 4 1500-lumen underwater lightings are installed to provide enough camera background light. Corresponding image processing and motion tracking code has been successfully developed to capture and follow the trajectory of either white or black markers. The following Fig.3 demonstrates a sketch of the general camera setup in the experiment and a sample of the raw and processed image of one of the ten cameras.

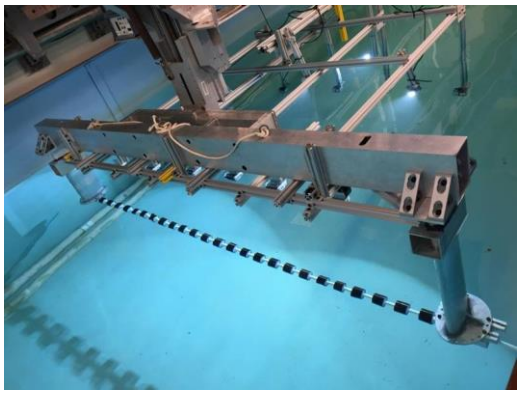

Fig.2 Experimental setup of riser model with 100% coverage buoyancy modules in the MIT Tow Tank

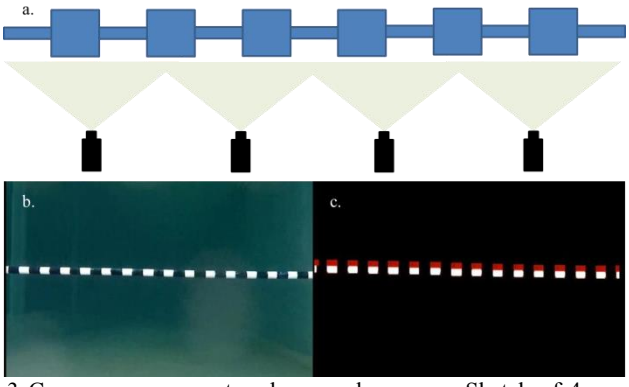

Fig.3 Camera arrangement and a sample case: a. Sketch of 4 camera coverage of the riser model in the CF direction, overlapping of each camera images will be used in the spatial synchronization; b. Sample image from one camera for the CF measurement; c. Processed image of Fig.3 b with image processing and motion tracking algorithm (the red bounding box shows the ability to capture and follow the motion of the white markers)

PRESENTATION OF DATA AND RESULTS: FULL COVERAGE

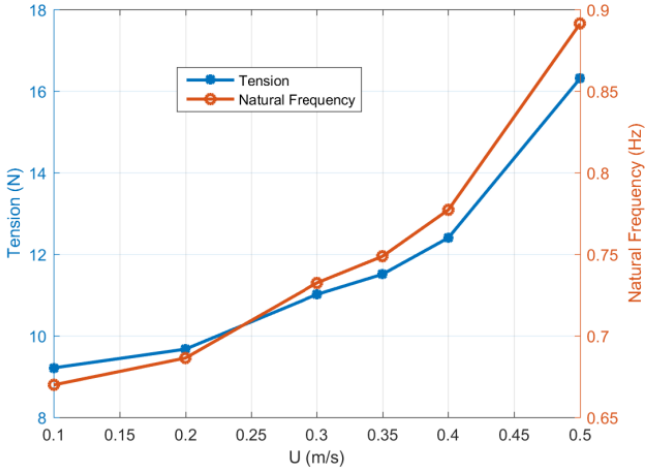

Fig.4 Tension (blue) and calculated fundamental natural frequency (red) V.S. flow velocity (riser with full coverage buoyancy module)

Six different velocities has been tested in the riser with full coverage buoyancy module experiment, which are 0.1m/s, 0.2m/s, 0.3m/s,

0.35m/s, 0.4m/s and 0.5m/s. And because of the fixed-fixed setup, the tension will increase with the increase of the velocity, and hence the rise fundamental natural frequency. The above Fig.4 shows the change of the tension and calculated natural frequency (assuming added mass coefficient C_m to be 1.0) with flow velocity.

Frequency Components Analysis on the CF Vibration.

FFT analysis is first performed along the model (A sample of the oscillation data over time at 9 different positions along the model is shown in the Fig.5), and later the major excitation frequency can be identified through the peak in the power spectral density (PSD) plot.

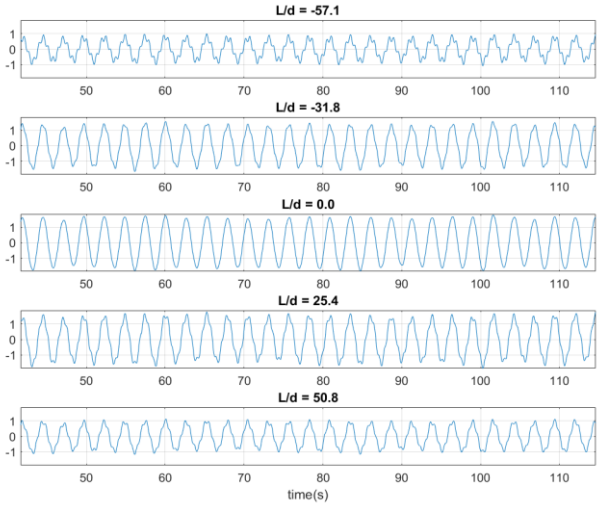

Fig.5 Sample oscillation data at 5 different positions along the model of full coverage for U = 0.1m/s.

Fig.6 displays the corresponding PSD of the data at 9 different postions along the model of full coverage at U = 0.1m/s. Clearly two different peaks of frequencies at 0.388Hz and 1.64Hz can be identified. The ratio between two is 4.2, and hence not an integer. The low frequency component of 0.388Hz is excited by the buoyancy modules, namely the larger diameter cylinder, while the high frequency component of 1.64Hz is contributed from the bare riser part.

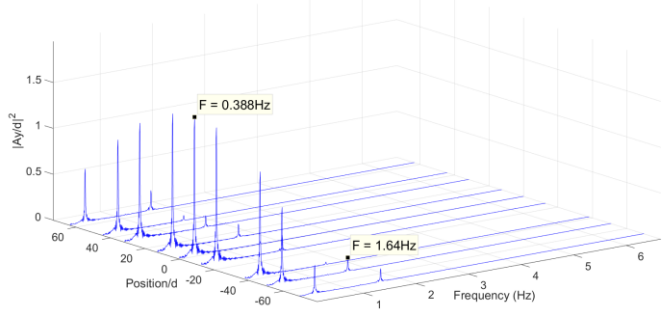

Fig. 6 PSD of displacement at 9 different position of the full coverage model (U = 0.1m/s)

Fig. 7 displays another PSD result of full coverage model at different velocity of U = 0.3m/s. Again both low and high frequency components can be identified, corresponding to both the buoyancy modules and riser contribution. However, for U = 0.3m/s case, at the low frequency range, we find two close frequency components of 0.732Hz and 1.03Hz. Later in the time-displacement analysis and time-frequency analysis, it will be revealed that these two close frequencies are due to the buoyancy module induced vibrational modal switch.

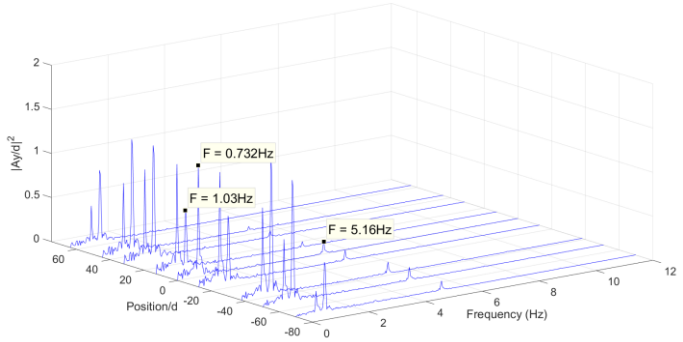

Fig. 7 PSD of displacement at 9 different positions of the full coverage model (U = 0.3m/s)

The coexistence of the low and high frequency components can be found for all the current experiments, so this means for the riser of full coverage of low-span-to-diameter-ratio buoyancy module, buoyancy module and riser will both contribute to the system vibration.

Picking out the peak frequencies, we plot the reduced frequency *Fr* (using small diameter in *Fr = fd/U* for high frequency component and using large diameter in *Fr = fD/U* for low frequency component) against flow velocity, shown in Fig. 8. As for the *Fr* of the riser motion, it remains a relatively constant value close to 0.20, which is slightly larger to the bare cylinder VIV motion around 0.14 – 0.16, as shown by Rao, et al. (2013). However, there is a surprising result of very low reduced frequencies for the buoyancy module contribution that the average value is around 0.11 but for the double low frequency cases (0.30m/s to 0.40m/s), the minimum value is only 0.085. The physical reason behind that still remains unclear and calls for a more detailed examination through future research including flow visualization. But this may be due to the fact that the finite length of the buoyancy module (aspect ratio is 1.0) will change the vortex shedding pattern a lot.

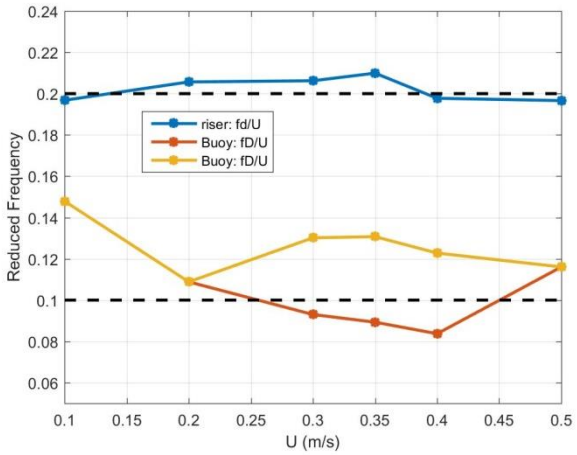

Fig.8 Reduced frequency for riser and buoyancy module component of model of full coverage

More importantly, it delivers us an important massage that when we construct the VIV hydrodynamic coefficient database by forced rigid cylinder vibration experiment, we need to extend one of the experiment parameter, reduced velocity *Ur* (inverse of the *Fr* described here in the Fig. 8) from normally 4-10 [3] to an even larger number of at least 12.

In the Fig.9, it displays the PSD result of both CF (blue) and IL (red) vibration for the full coverage model at U = 0.2m/s. the IL displays a

mono-frequency vibration at 1.16Hz, twice of the CF buoyancy module contribution, and yet, second harmonic of the riser CF vibration frequency is not found in the IL direction for the current experiment at U = 0.2 m/s.

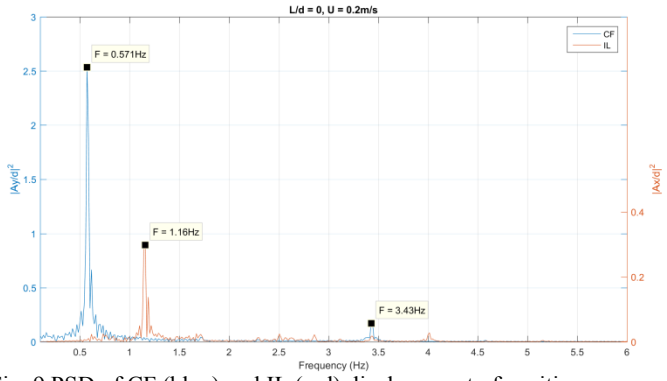

Fig. 9 PSD of CF (blue) and IL (red) displacement of position *L/d = 0* for full coverage model at U = 0.2m/s

Separation of the Multi-Frequency Vibration.

After the identification of the multiple frequencies in the CF direction due to the riser and buoyancy module staggered configuration, it is naturally to ask the following questions

1. What kind of mode will the riser vibrate in, or more precisely will multiple modal vibrations be excited due to the multiple frequency external loading?
2. Does these multiple frequency / modal vibration exist at the same time or do they vibrate in a different time period?

As if this is the case, again in the rigid forced vibration experiment, we need to reevaluate the parameters for the experiment in order to better understand and provide a more completed hydrodynamic database. Instead of a single frequency sinusoidal motion trajectory, multiple frequency and amplitude motion trajectory should be applied.

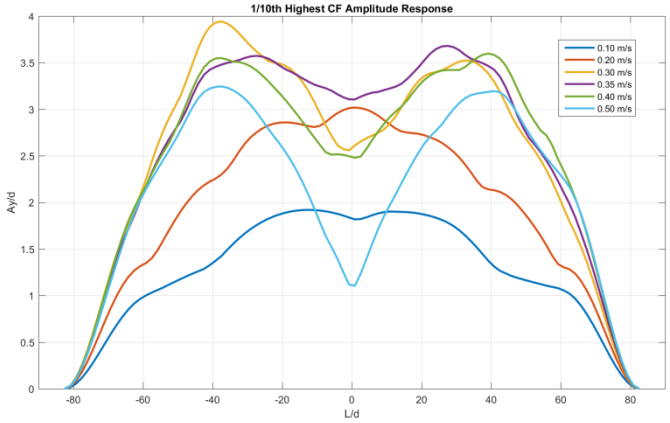

Fig. 10 1/10th highest *CF* amplitude response of full coverage model for U = 0.1m/s to 0.5m/s

The 1/10th highest response of the CF vibration is calculated for all the experimental cases from 0.1m/s to 0.5m/s and shown in the above Fig. 10. We can first observe that the model exhibits large CF vibration amplitude, reaching almost 4 riser diameter (1.3 buoyancy module diameter) at U = 0.30m/s, and this suggests that in the full coverage model experiment, the buoyancy module induced VIV dominates the riser CF amplitude response. Second of all, the result shows that starting with the first modal vibration for 0.1m/s and 0.2m/s due to the excitation of low frequency of buoyancy module, the riser will start to exhibit overall second modal vibration when the flow velocity increase in the current experiment. Besides, we also see small "ripples", such as in 0.1m/s and 0.2m/s case, on top of the overall the large low modal response, which is corresponding to the existence of the high frequency / modal response.

Band pass filter is applied to the data along the model to separate different frequency vibration component. In the Fig. 11, it shows the total CF response, separated low frequency CF response and high frequency CF response for the full coverage model at U = 0.1m/s. It reveals that the low modal (1st) vibration occupies the majority of the amplitude response, while the 4th mode is also being excited due to the riser high frequency contribution. Therefore here is clear evidence that due to the multiple-frequency loading. Risers with buoyancy modules will exhibit a multiple modal vibration behavior.

Apart from the 1/10th highest CF response, in the following Fig. 12, we plot the riser time displacement of the total response, separated low frequency response and high frequency response in CF direction with same time period for U = 0.1m/s. The result shows the fact that low frequency response indeed dominates the total response, hence the similarity between the total and low frequency response. And at the same time, it also answers the question that the multiple frequency / modal vibration of the riser of buoyancy module coexists simultaneously.

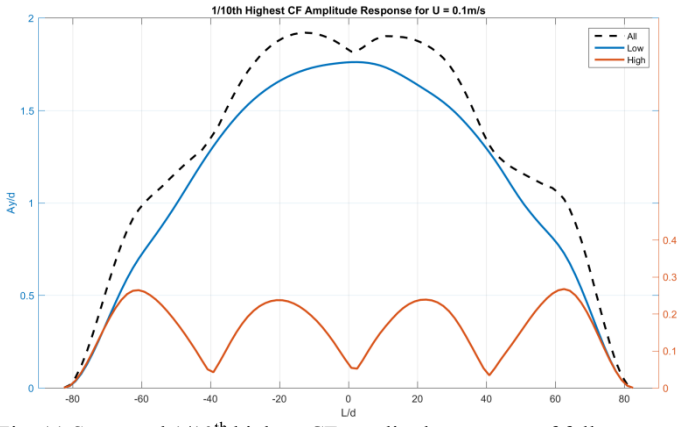

Fig. 11 Separated 1/10th highest CF amplitude response of full coverage model for U = 0.1m/s (dash line: total response; blue line: low frequency buoyancy module induced response; red line: high frequency riser induced response).

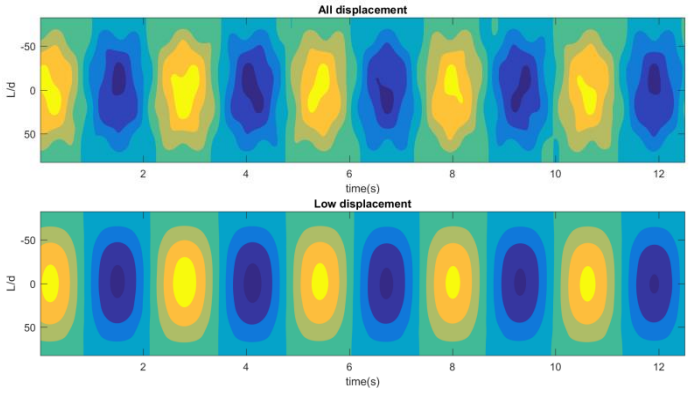

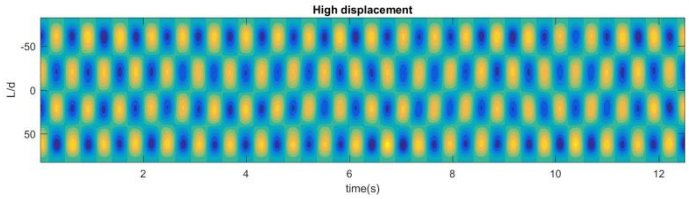

Fig. 12 CF time displacement of the full coverage model for U = 0.1m/s (Top: total displacement response; Middle: low frequency displacement response; Bottom: High frequency displacement response)

Another phenomenon we address here is the double low frequencies for U = 0.3m/s, 0.35m/s and 0.4m/s cases. Here we in the Fig. 13, we plot the riser CF low frequency time displacement, the time history of the CF vibration at position *L/d = -34.2* and the wavelet synchronization transformation of the data at position *L/d = -34.2* for U = 0.4m/s. Here we can see that before 6s, the time displacement of the riser CF vibration displays an unstable (1st and 2nd mode mixing) vibration, where the time history of the CF vibration at *L/d = -34.2* displays an irregular vibration before 8s. And after 8s, at *L/d = -34.2* the motion becomes more regular, while the riser response in a more stable 2nd modal vibration. This is also supported by the wavelet synchronization transformation that the time-frequency information is revealed. Before s, apart from the dominating 1.29Hz component, another 0.85Hz also provides a visible contribution, while after 8s, its energy becomes much weaker, and hence the more regular motion at position *L/d = -34.2* and the 2nd stable modal riser vibration.

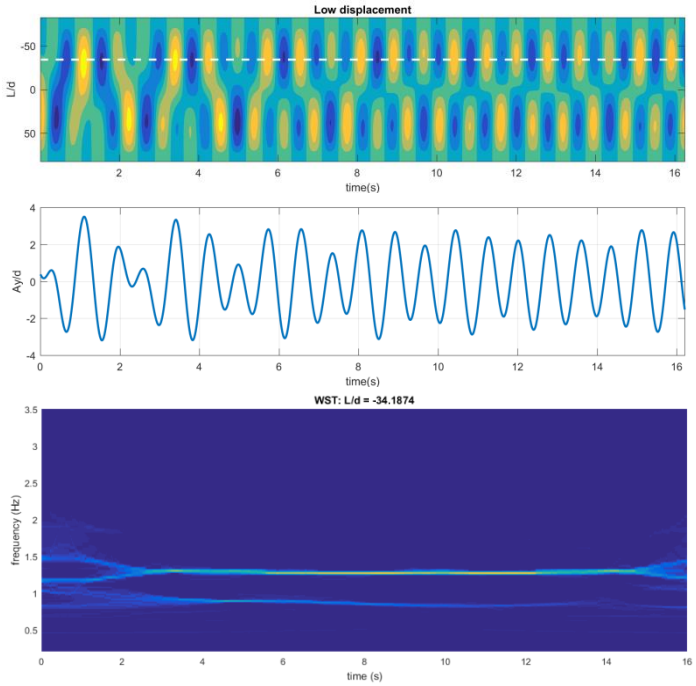

Fig. 13 Time frequency analysis of full coverage model at U = 0.4m/s (Top: low frequency displacement response, the white line is *L/d = -34.2*; Middle: vibration response at position of *L/d = -34.2*; Bottom: wavelet synchronization transformation at the position of *L/d = -34.2*).

***Combined CF and IL Vibration: Fig. 8 Motion*:**
As studied by Dahl (2008) and Bourguet, et al. (2013), the phase angle, amplitude ratio, etc. of CF and IL motion are the keys to determine the system VIV properties, such as the energy transfer direction between fluid and structure. In this section, we will focus on the combined CF and IL vibration of the model.

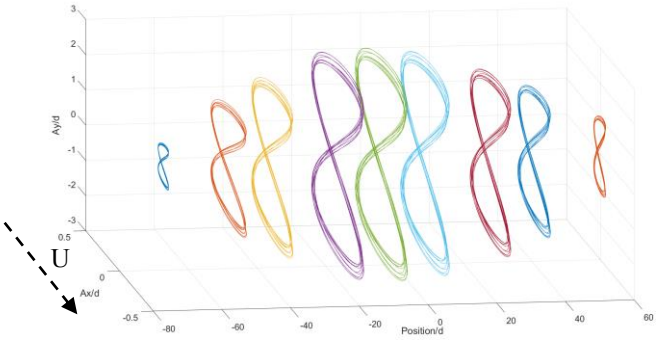

Fig. 14 CF and IL combined motion for low frequency component along the entire full coverage model at U = 0.2m/s

In the current experiment, because of the excitation from both buoyancy module and riser section, there are multiple frequencies in both CF and IL direction, here we will again use band pass filter to pick CF motion by the peak in the PSD plot, and corresponding second harmonic frequency range will be selected for the IL motion. Here in the Fig. 14 of CF and IL combined motion for the low frequency component for the full coverage model at U = 0.2m/s, the direction of the arrow represents the flow velocity. And in the Fig. 15, CF and IL combined at different position are displayed with the red arrow displaying the direction of the Fig. 8 trajectory. Here we can see that at U = 0.2m/s, along the riser span, the buoyancy module induced motion displays coherent counter-clockwise motion, which indicting a high possible energy-in from the fluid to structure (positive Clv), and hence explains the large buoyancy module dominated response.

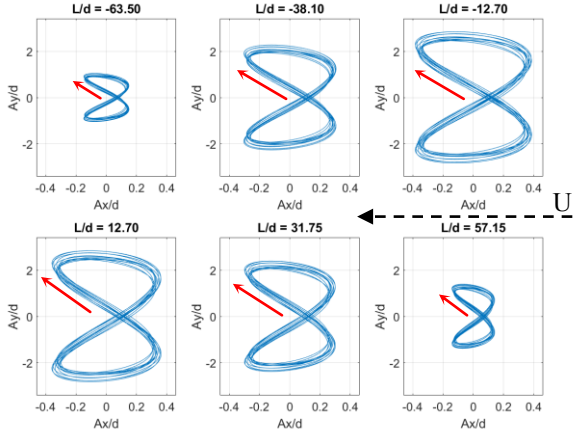

Fig. 15 CF and IL combined motion for low frequency component on 6 different positions at U = 0.2m/s

Same as in the analysis of the buoyancy module induced motion, riser induced high frequency CF and IL combined motion all along the model is picked out and plotted in the Fig. 16 and 6 representatives are selected for different position along the riser model. Unlike the coherent counter-clockwise buoyancy induced motion all along the model, clear orbit drifting can be identified, and hence the messier trajectory. However, still we can observe a general CF and IL orbit pattern that as for the riser induced high frequency motion, both clockwise and counter-clockwise figure-8 motions is observed, and this indicts that both energy in and out exists for the riser induced motion.

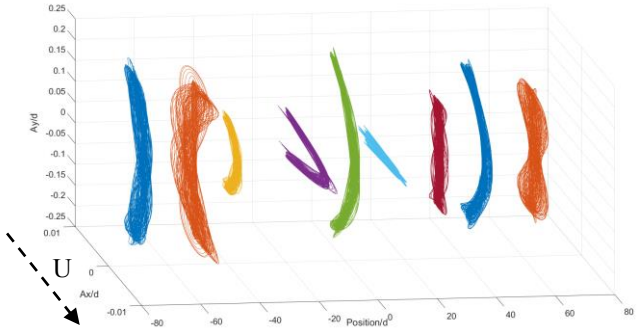

Fig. 16 CF and IL combined motion for high frequency component along the entire full coverage model at U = 0.2m/s

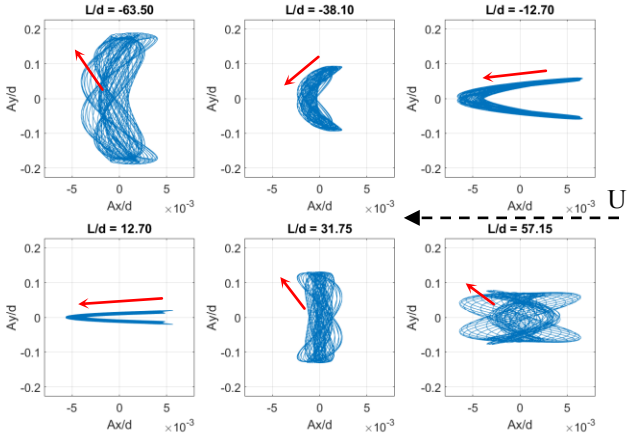

Fig. 17 CF and IL combined motion for high frequency component on 6 different positions at U = 0.2m/s

Added Mass Variation in the CF and IL Vibration: an Comparison between Flexible Model and Rigid Model Experiment

In the following Fig. 18, it shows the RMS value of the CF and IL response of the full coverage model at U = 0.2m/s. We can see that both CF and IL both display 1st modal vibration, instead of 2nd modal for IL vibration, which is expected since the main IL buoyancy module excitation frequency is twice to that of the CF direction. And in the Fig. 19, we plot the RMS value of the CF low and high frequency response, where we can identify the 7th modal riser induced vibration.

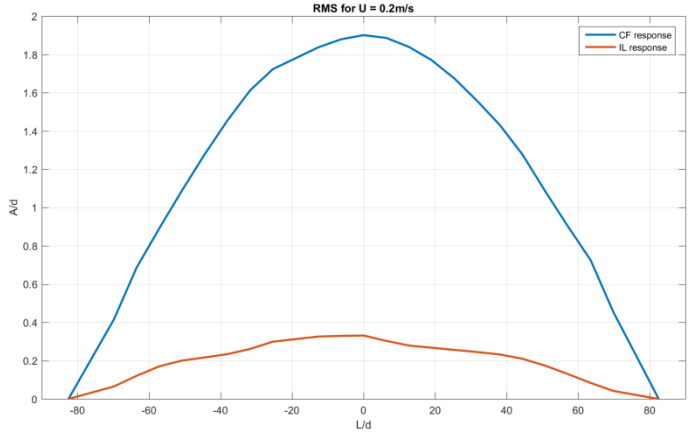

Fig. 18 RMS of the CF (blue) and IL (red) response of full coverage model at U = 0.2m/s

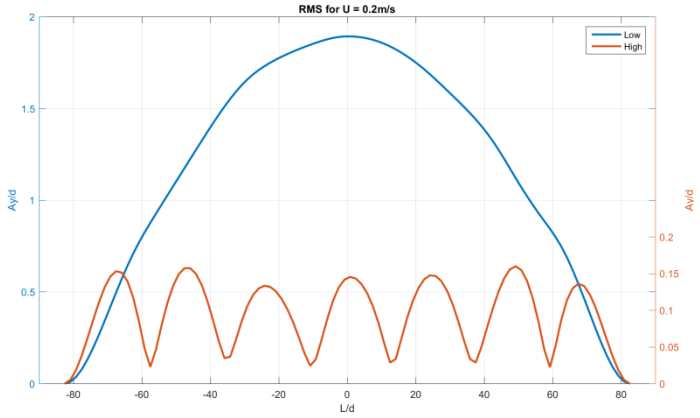

Fig.19 RMS of the CF low frequency (blue) and high frequency (red) response of full coverage model at U = 0.2m/s

From the analysis of the combined CF and IL motion, and based on the calculated phase angle between the CF and IL, we are able to link the flexible model response with the hydrodynamic coefficient acquired by the rigid model forced vibration experiment. Le Garrec, et al. (2016) has performed and experiment of the rigid riser model with low-span-to-diameter-ratio buoyancy module. In the Fig. 20, the star picked out the added mass coefficient for the CF and IL direction for the corresponding buoyancy module and riser induced motion for the case of U = 0.2m/s. It reveals that the IL added mass coefficient C_{mx} = -0.6, and CF added mass coefficient C_{my} = 0.85 for the buoyancy module induced motion, and C_{my} = 2.65 for the riser induced motion. And this results in different natural frequencies for the 1st mode in CF and IL direction (IL: F_{nI} = 1.283 Hz, F_{IL} = 1.16 Hz; CF: F_{nI} = 0.64Hz, F_{CF} = 0.57Hz).

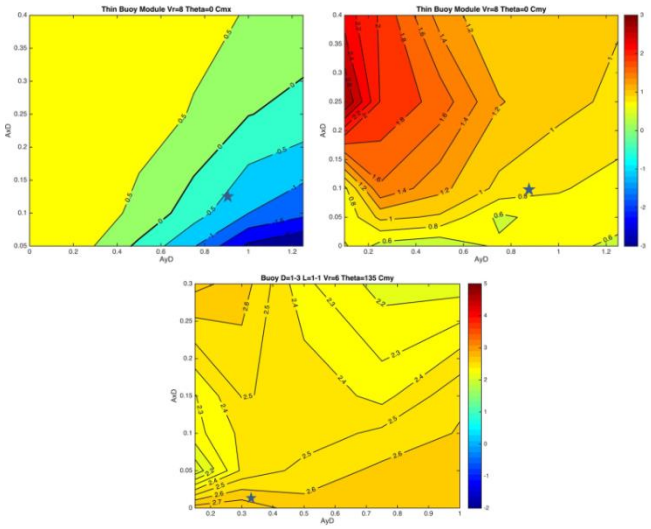

Fig. 20 Added mass coefficient acquired via rigid model forced vibration (Top left: IL added mass coefficient C_{mx} for phase angle of 0° at buoyancy module based Vr = 8; Top right: CF added mass coefficient C_{my} for phase angle of 0° at buoyancy module based Vr = 8; Bottom: CF added mass coefficient C_{my} for phase angle of 135° at riser based Vr = 6;)

PRESENTATION OF DATA AND RESULTS: HALF COVERAGE

Riser model of buoyancy module with half coverage has also been tested for the same 6 velocities as the full coverage experiment from

0.1m/s to 0.5 m/s. The sample vibration data is shown in the following Fig. 21. For all the following plots, we follow the convention that buoyancy module is in the positive L/d range, and riser is in the negative L/d range.

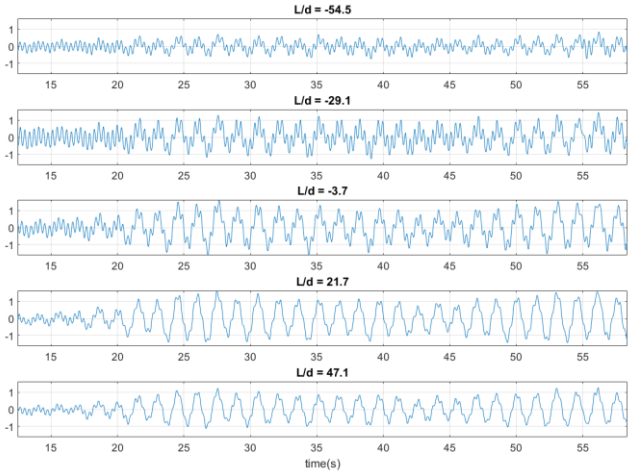

Fig.21 Sample oscillation data at 5 different positions along the model of half coverage for U = 0.2m/s.

Frequency and Amplitude Analysis

The result of the PSD of the displacement of the U = 0.2m/s and U = 0.35m/s is shown in the Fig. 22 and Fig. 23. Same as in the full coverage model, half coverage also displays a bi-frequency response excited from both riser and buoyancy module. However in the half coverage case, because riser section has a larger exposure length, the response of the riser and buoyancy module is comparable in amplitude, or in some case, riser acquired a stronger response, shown in the Fig. 23 for U = 0.35m/s.

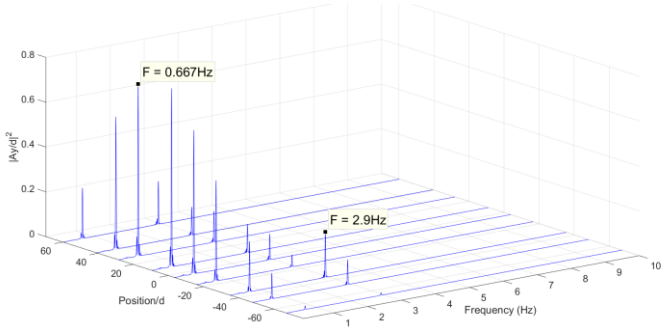

Fig. 22 PSD of displacement at 9 different position of the half coverage model (U = 0.2m/s)

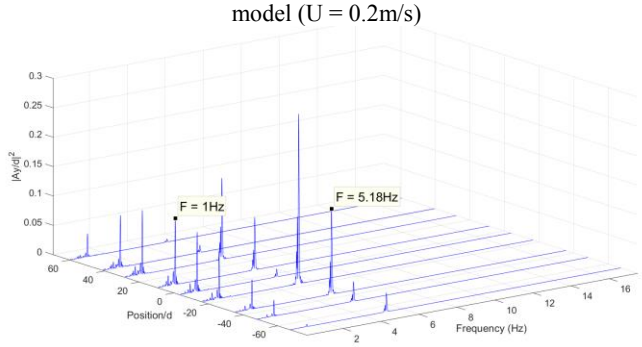

Fig. 23 PSD of displacement at 9 different position of the half coverage model (U = 0.35m/s)

The peak frequency in the PSD plot is picked out and plotted as the reduced frequency V.S. the flow velocity in the Fig. 24. In the model of half coverage, the riser induced VIV motion is on averagely 0.17 for the reduced frequency, while again we observe a relatively low reduced frequency for the buoyancy module induced motion (except for the U = 0.1m/s case, where riser completely dominates the total response and suppresses the buoyancy module induced motion.).

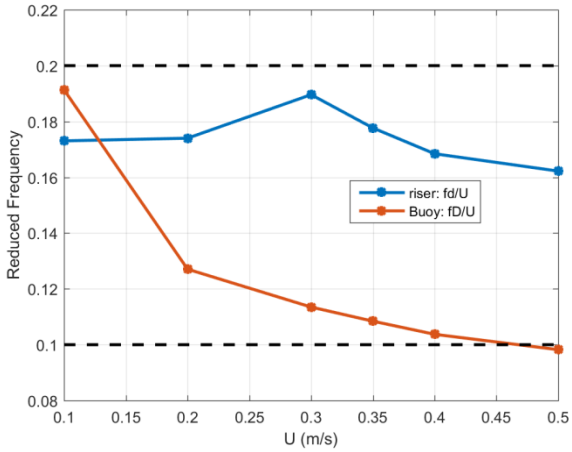

Fig. 24 Reduced frequency for riser and buoyancy module component of model of half coverage

The 1/10th highest CF amplitude response for all experimental cases are plotted in the Fig. 25. As we can see, the largest amplitude response is less than 2.5d for the U = 0.5m/s case, which is much smaller than that of the full coverage model. This suggests that the larger coverage ratio may result in a larger amplitude response which is due to stronger buoyancy module contribution. Also, compared to the full coverage model, we can see from the Fig. 10 and Fig. 25 that because of the smaller coverage ratio, riser induced motion will have a much stronger effect on the total amplitude response for the model of half coverage.

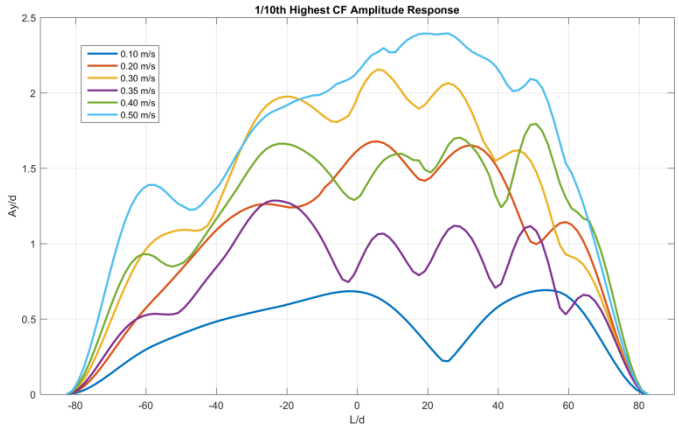

Fig. 25 1/10th highest *CF* amplitude response of half coverage model for U = 0.1m/s to 0.5m/s

Bandpass filter is then applied based on peaks in the PSD analysis to separate the buoyancy module induced low frequency vibration and riser induced high frequency vibration. And the result of the U = 0.2m/s and U = 0.5m/s is plotted in the Fig.26 and Fig. 27. Here we can see that the buoyancy module induced 1st modal-like vibration for both 0.1m/s and 0.5 m/s case and its largest amplitude is shifted from middle to the positive (buoyancy module covered) range. As for the riser induced motion, because of the larger mass per unit, wave length is hence smaller in the buoyancy module covered area, compared to the bare riser area. One interesting phenomenon we found for all the

experimental case is that the amplitude of the riser induced motion decreases when it goes further into the buoyancy module covered area. This suggested that the buoyancy module low frequency motion may help to mitigate the high frequency riser induced motion and prevent its energy from traveling further.

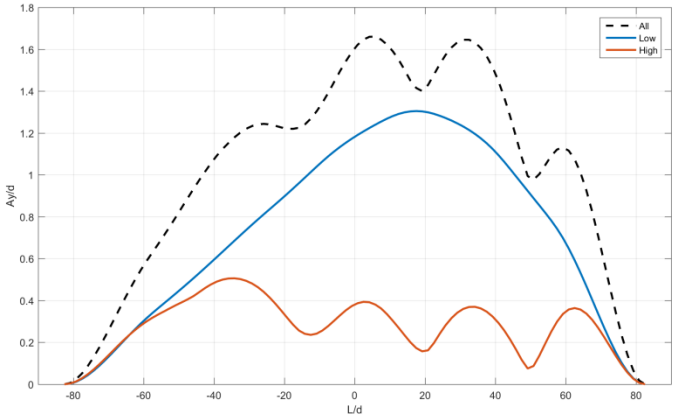

Fig. 26 Separated 1/10th highest CF amplitude response of half coverage model for U = 0.2m/s (dash line: total response; blue line: low frequency buoyancy module induced response; red line: high frequency riser induced response).

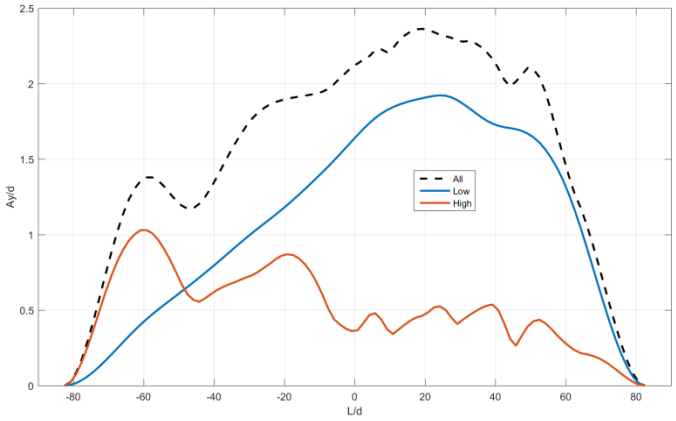

Fig. 27 Separated 1/10th highest CF amplitude response of half coverage model for U = 0.5m/s (dash line: total response; blue line: low frequency buoyancy module induced response; red line: high frequency riser induced response).

***Buoyancy Module and Riser Induced Traveling Wave*:**
Because of the half buoyancy module covered setup on one side, riser induced motion will form traveling waves from bare riser side to the buoyancy module covered side. In the figure 28, we plot the time displacement for the total response, low frequency buoyancy module induced response and also the high frequency riser induced response. We can see that due to the traveling wave pattern and the multiple frequency response, the total response is "messy". Yet from the low frequency and high frequency component time displacement, regular vibration pattern can be clearly identified that for the low frequency buoyancy module induced motion (Fig. 28 b), it exhibits the first modal vibration with largest amplitude shifted to the buoyancy module covered side (positive range). And for the high frequency, the arrow is drawn showing the direction of the traveling wave from the bare riser section to the buoyancy module covered section.

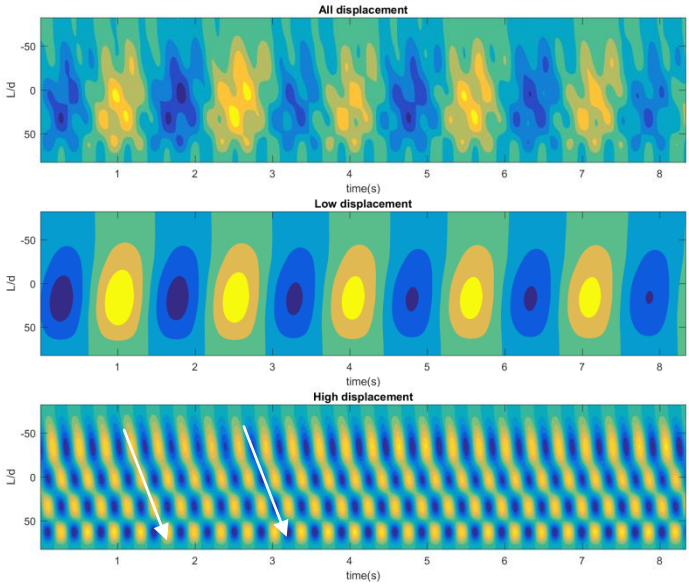

Fig. 28 CF time displacement of the half coverage model for U = 0.2m/s (Top: total displacement response; Middle: low frequency displacement response; Bottom: High frequency displacement response)

The following Fig. 29 shows the total CF and IL combined motion for the half coverage at U = 0.2m/s. The result again is "messy" for both CF and IL direction, and hence the CF and IL trajectory and their phase angle cannot be easily identified.

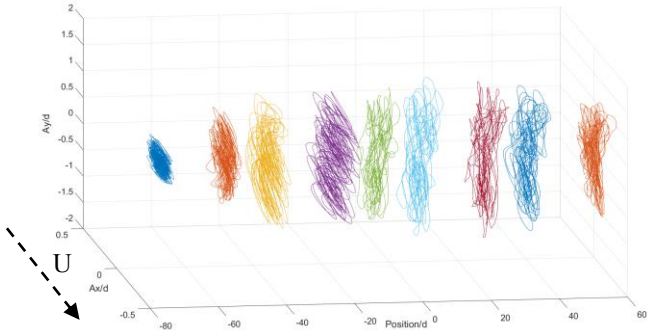

Fig. 29 CF and IL combined motion along the entire half coverage model at U = 0.2m/s (the response is "messy" due to the traveling wave and multiple frequency response)

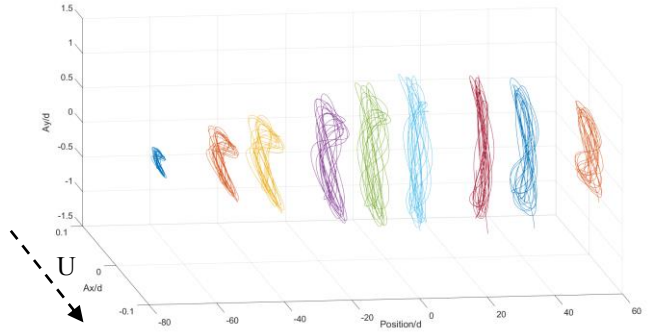

Fig. 30 CF and IL combined motion for low frequency component along the half coverage model at U = 0.2m/s

Same as in the Fig. 14 and 15, the buoyancy module induced motion was picked out through bandpass filter, and plotted in the Fig. 30 and 31 for half coverage model at U = 0.2m/s. It shows that in the buoyancy module covered area, the counter-clockwise CF and IL figure 8

trajectory can be observed, and this indicts the possible energy in region for the low frequency motion. At the same time, no coherent low frequency trajectory can be observed in the riser range, which explains the shift of the largest amplitude for the buoyancy induced 1st mode.

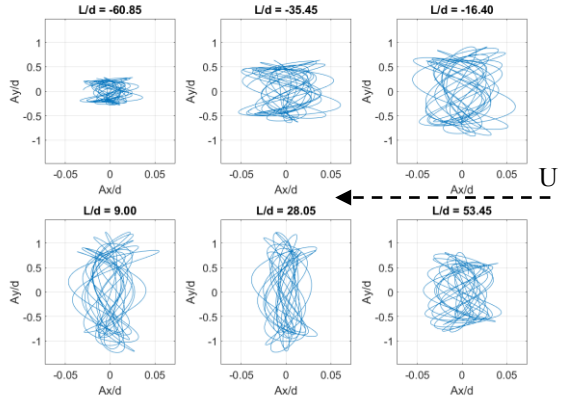

Fig. 31 CF and IL combined motion for low frequency component on 6 different positions at U = 0.2m/s

The CF and IL riser induced motion is plotted in the following Fig. 32 and 33. We can observe coherent figure-8 motion along the entire model, and however the direction of the figure-8 motion changes along the span. We can see in the Fig. 33 that in the bare riser section, model displays counter-clockwise motion, while at the buoyancy module covered section, coherent clockwise motion is observed. Such motions suggest a high energy in possibility in the bare riser section and an energy out in the buoyancy module covered section for the riser induced high frequency motion, and there this explains the amplitude decrease of the high frequency component in the buoyancy module covered section.

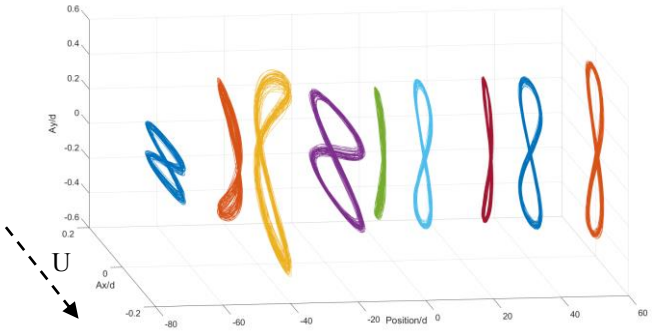

Fig. 32 CF and IL combined motion for high frequency component along the half coverage model at U = 0.2m/s

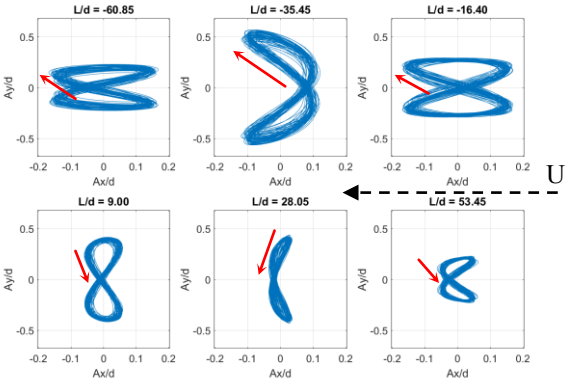

Fig. 33 CF and IL combined motion for high frequency component on 6 different positions at U = 0.2m/s

CONCLUSIONS

In the current research, riser with buoyancy modules (module aspect ratio of 1.0) has been experimentally studied for both 100% and 50% coverage ratio. The result shows that both buoyancy module and bare riser will contribute and therefore result in a multiple frequency / modal vibration. However for buoyancy module, its induced vibration will experience a relatively low value down to 0.085, and this suggests an extension of the reduced velocity for the rigid model based hydrodynamic database. Besides, compared CF & IL combined motion with the rigid cylinder measured hydrodynamic coefficient, large added mass coefficient variation is identified as the cause for the natural frequency and mode change. Besides, in the half coverage model experiment, the amplitude of the riser induced high frequency motion will decrease in the buoyancy module covered section, associated with a CF and IL clockwise trajectory.

REFERENCES

Bourguet, R., Karniadakis, G. E., and Triantafyllou, M. S. Phasing mechanisms between the in-line and cross-flow vortex-induced vibrations of a long tensioned beam in shear flow. *Computers & Structures*, 122, 155-163, 2013.

Dahl, J. J. M. Vortex-induced vibration of a circular cylinder with combined in-line and cross-flow motion (*Doctoral dissertation, Massachusetts Institute of Technology*). 2008.

Fan, D., Du, H., and Triantafyllou, M. S. "Optical Tracking Measurement on Vortex Induced Vibration of Flexible Riser with Short-Length Buoyance Module." *Bulletin of the American Physical Society 61*, 2016.

Javadi, K., and Kinai, F. On the Turbulent Flow Structures over a Short Finite Cylinder: Numerical Investigation, 2014

Jhingran, V., Zhang, H., Lie, H., Braaten, H., and Vandiver, J. K. (2012, April). Buoyancy Spacing Implications for Fatigue Damage due to Vortex-Induced Vibrations on a Steel Lazy Wave Riser (SLWR). In *Offshore Technology Conference*. Offshore Technology Conference, 2012

Le Garrec, J., Fan, D., Wu, B., and Triantafyllou, M. S. (2016, December). Experimental investigation of cross flow-inline coupled Vortex-Induced Vibration on riser with finite length buoyancy module. In *OCEANS 2016 MTS/IEEE Monterey*. IEEE, 2016.

Li, L., Fu, S., Yang, J., Ren, T., and Wang, X. Experimental investigation on vortex-induced vibration of risers with staggered buoyancy. In *ASME 2011 30th International Conference on Ocean, Offshore and Arctic Engineering* (pp. 51-59). American Society of Mechanical Engineers, 2011.

Halvor, L., Mo, K., and Vandiver, J. K. "VIV model test of a bare-and a staggered buoyancy riser in a rotating rig." *Offshore Technology Conference*. Offshore Technology Conference, 1998.

Rao, Z., Vandiver, J. K., and Jhingran, V. "VIV excitation competition between bare and buoyant segments of flexible cylinders." *ASME 2013 32nd International Conference on Ocean, Offshore and Arctic Engineering*. American Society of Mechanical Engineers, 2013.

Triantafyllou, M. S., Triantafyllou G. S., Tein Y. S., and Ambrose B.D. "Pragmatic riser VIV analysis." *Offshore technology conference*. Offshore Technology Conference, 1999.

Vandiver, J. K., and Peoples, W. "The effect of staggered buoyancy modules on flow-induced vibration of marine risers." *Offshore Technology Conference*. Offshore Technology Conference, 2003.

Xu, Y., Fu, S., Chen, Y., Zhong, Q., and Fan, D. "Experimental investigation on vortex induced forces of oscillating cylinder at high Reynolds number." *Ocean Systems Engineering 3, no. 3* (2013): 167-180.